A Revertible, Autonomous, Self-Assembled DNA-Origami Nanoactuator

ARTICLE *in* NANO LETTERS · NOVEMBER 2011

Impact Factor: 13.59 · DOI: 10.1021/nl203217m · Source: PubMed

NANO LETTERS

LETTER

pubs.acs.org/NanoLett

A Revertible, Autonomous, Self-Assembled DNA-Origami Nanoactuator

Monica Marini,[†] Luca Piantanida,[‡] Rita Musetti,[†] Alpan Bek,[‡,¶] Mingdong Dong,[§] Flemming Besenbacher,[§] Marco Lazzarino,[‡,∥] and Giuseppe Firrao*[,†,⊥]

[†]Dipartimento di Scienze e Agrarie ed Ambientali, Università degli Studi di Udine, via delle Scienze 208, 33100 Udine, Italy

[‡]CBM scrl Area Science Park — Basovizza, 34149 Trieste, Italy

[§]Center for DNA Nanotechnology (CDNA), Interdisciplinary Nanoscience Center (iNANO) and Department of Physics and Astronomy, Aarhus University, DK-8000 Aarhus, Denmark

[∥]IOM-CNR-Laboratorio TASC, Area Science Park — Basovizza, 34149 Trieste, Italy

[⊥]INBB Istituto Nazionale di Biostrutture e Biosistemi, Interuniversity Consortium, Italy

Supporting Information

ABSTRACT: A DNA-origami actuator capable of autonomous internal motion in accord to an external chemical signal was designed, built, operated and imaged. The functional DNA nanostructure consists of a disk connected to an external ring in two, diametrically opposite points. A single stranded DNA, named probe, was connected to two edges of the disk perpendicularly to the axis of constrain. In the presence of a hybridizing target molecule, the probe coiled into a double helix that stretched the inner disk forcing the edges to move toward each other. The addition of a third single stranded molecule that displaced the target from the probe restored the initial state of the origami. Operation, dimension and shape were carefully characterized by combining microscopy and fluorescence techniques.

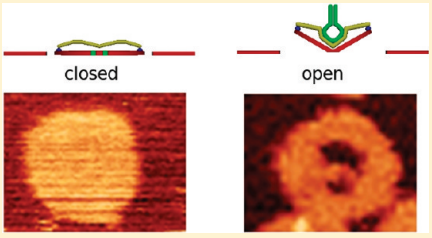

KEYWORDS: DNA origami, self-assembly, autonomous switch, reusable, actuation

A major challenge in the development of intelligent nanodevices is to endow with the ability to perform desired actuation and motion at the nanoscale. Although motion with atomic resolution has been achieved by top-down fabrication using the piezoelectric properties of materials, bottom up fabrication of devices capable of controlled motion is still confined to a few examples, most of which based on natural biological molecular motors.[1] In a few examples, the dynamic properties of DNA have been exploited to obtain simple motors,[2,3] as DNA may change its structure in a highly controlled manner according with the strands' interaction occurring in the formation of the double helix. Indeed, the specificity of Watson and Crick base pairing in the DNA not only determines the chemical foundation for genetics, but also confers predictable conformational properties that make this nucleic acid a suitable material for the assembly of highly structured materials with specific features.[4] As far as static constructs are concerned, the DNA-Origami technique, introduced by Rothemund[5] has become a powerful scheme in the field of DNA nanotechnology, allowing the construction of two-dimensional (2D)[5,6] or three-dimensional (3D)[7,8] complicated nanoscale objects. This method relies on the folding of a long single-stranded polynucleotide named "scaffold strand" with hundreds of short synthetic oligonucleotides named "staple strands" to create arbitrary and precise shapes defined by the staple sequences' choice. Since then, the designed 2D objects were modified in different ways with nanometer precision using the DNA-based surface as a platform to address single molecule detection,[9] chemical reactions,[10] and nanomaterials.[11] Moreover, the short oligonucleotides can be chemically modified in several ways to link functional molecules and can be used directly as staple strands or via hybridization to an oligomer protruding on the upper or lower surface of the planar origami. On the basis of this principle, patterns of inorganic materials were created with gold[12] and silver[13] nanoparticles, or even with biological molecules such as streptavidin and other proteins with the purpose of developing nanoplatforms for enzymatic reactions[10] and regularly ordered nanoarrays.[14] The design of complex 3D DNA origami-based shapes is evolving rapidly: 3D oriented origami were developed combining multiple curved elements, where in a single scaffold molecule, targeted insertions and deletions of base pairs cause the DNA bundles to develop twist of either handedness or to curve in a quantitatively controlled manner.[15] With this method Dietz and co-workers[15] created a number of helix bundles programmed to have a precise degree of bending, spirals with a unique scaffold strand, half circles wheels and several other complex shapes.[15] In this way, a number of static nanostructures have been developed through either one step hybridization assembly process or via a sequential assembly process along with independently preassembled DNA sub-blocks, demonstrating that effective design using the bottom-up approach to build nanostructures at the nanoscale has

Received: September 15, 2011
Revised: November 1, 2011
Published: November 03, 2011

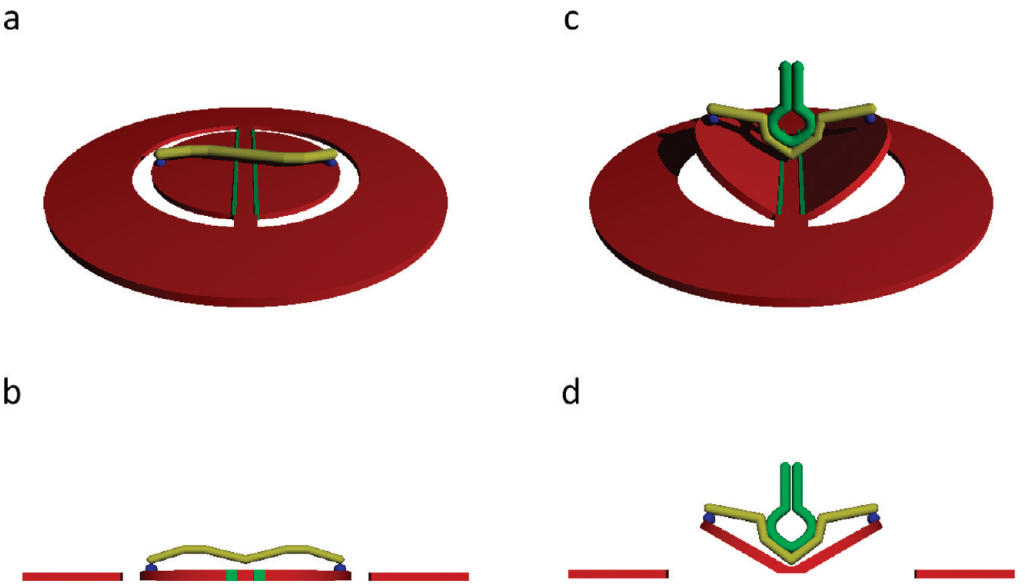

Figure 1. Schematic model of the DNA-origami. As represented, the origami is made of two main subunits, an external ring and an internal disk constrained in two opposite points to the external ring. The flexibility of the internal disk is guaranteed by a four noncomplemented nucleotide spacer (green lines). (a,b) Upper and lateral view of a closed DNA-origami with a noncomplemented single stranded probe. (c,d) Upper and lateral view of an actuated DNA origami; the probe (yellow) is complemented to the hairpin target molecule (green).

been achieved. Despite these structures can be precisely designed, they are generally static and capable of limited functional motion, being based on the irreversible alteration of the origami double helix structure,[7] and therefore not suitable for construction of a reversible actuator that could be integrated into more complex nanodevices. It would be highly desirable to construct an autonomous DNA-based object based on the origami platform with nanometer-sized structural modules, reacting to specific external signals, since this would open dynamic, visionary perspectives of transduction, elaboration, and integration of environmental signals and operator commands into nanomachines.

Here we indeed demonstrate the design of self-assembled DNA-origami nanostructures capable of an autonomous switchable motion and with an unique addressable change of conformation and shape in response to environmental stimuli provided by the operator. The mechanical motion of this DNA origami nanostructure is fully reversible, making use of the simple and well-known rules of base-pairing between different nucleic acids strands.

We have designed and produced 2D DNA circular objects of an estimated total diameter of ~100 nm, consisting of an internal disk of an estimated total diameter of ~60 nm and an external ring, of ~20 nm (shown schematically in Figure 1a). To obtain the desired shape, the entire single-stranded circular DNA of the M13mp18 viral genome (7249 nt) was self-assembled in solution with 218 synthetic oligonucleotides called "staple strands" in a single step synthesis process (Table S1 Supporting Information). The design of the DNA switch is achieved using the same strategy adopted in the traditional DNA origami method, that is, the single-stranded M13 DNA scaffold is designed to fold back and stretch to the opposite direction at the designed end point. Because the connection point was mechanically critical for the nanostructure, two independent subunits were constructed with a unique scaffold molecule, that is, an external ring and an internal disk that was connected to the ring in two opposite points. In order to secure flexibility to the two semihalves of the internal disk (named "wings") and thus allow them to bend relative to the plane of the ring, the DNA was left single stranded for a length of four nucleotides in each row of the internal disk in positions aligned to a row perpendicular to the bending axis of the wings, as shown in the Supporting Information (Figure 1). All the staples and the scaffold were mixed together and annealed in a thermocycler, slowly cooling the reactions. The synthesis resulted in a stable construct, that migrated in nondenaturing agarose gel electrophoresis as a unique and distinct sharp band (Supporting Information Figure S2), suggesting the formation of a homogeneous 2D DNA nanostructure.

Further structural information on the shape of designed DNA was gained with liquid phase atomic force microscopy (AFM) that directly revealed the formation of isolated DNA origami nanostructures with average diameter of 97 ± 6 nm and average height of 2.1 ± 0.2 nm. No double layers existed (Figure 2a) but a significant portion of origami nanostructures appeared to be connected on their side in couples (Figure 2b) probably due to blunt ends' interactions forces between the same edges. A detailed analysis on more than 2000 nanostructures revealed that 75 ± 2% of the disks adopted the designed shape while 25 ± 2% of the disks were incomplete, missing often the internal disk or part of the external ring (Figure 2d). Further AFM images are available as Supporting Information.

In order to control the motion of the DNA origami wings, two oligonucleotides of the internal disk were in a more complete design substituted with longer oligomers with sticky ends protruding on the upper face of the disk, on the edges of the two opposite movable wings. This modification allowed for linking in the self-assembly step of the "probe", a single-stranded DNA molecule designed to be 120 nts long with the ends complementary to the above-mentioned sticky ends. Moreover, the probe was constructed to be perfectly complementary to a hairpin nucleic acids named "target", as depicted in Figure 1b. The hybridization between the target and the probe nucleic acids and the consequent double stranded (ds) DNA formation, originates from a tensile force on the internal disk changing its

dx.doi.org/10.1021/nl203217m |*Nano Lett.* 2011, 11, 5449–5454

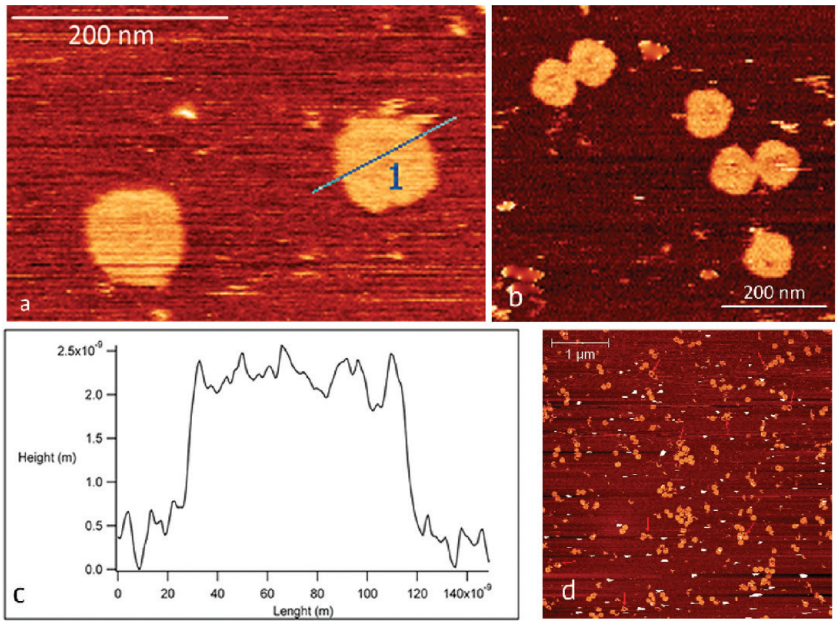

Figure 2. AFM imaging of DNA origami structures as formed, hybridized with the probe during the annealing step. (a) AFM image in tapping mode in liquid of two well-formed closed DNA origami and (c) height profile of the structure, referred to the line 1 in the AFM image. The profile analysis highlights the correspondence of the self-assembled nanostructure with the design dimensions: height around 2 nm and diameter around 100 nm. (b) AFM topographic image of well formed origami pairs originating from lateral blunt ends interaction. There is no opening between the inner disk and the outer ring. (d) Low-resolution AFM image showing incomplete DNA origami (red arrows), missing the internal disk and part of the external ring.

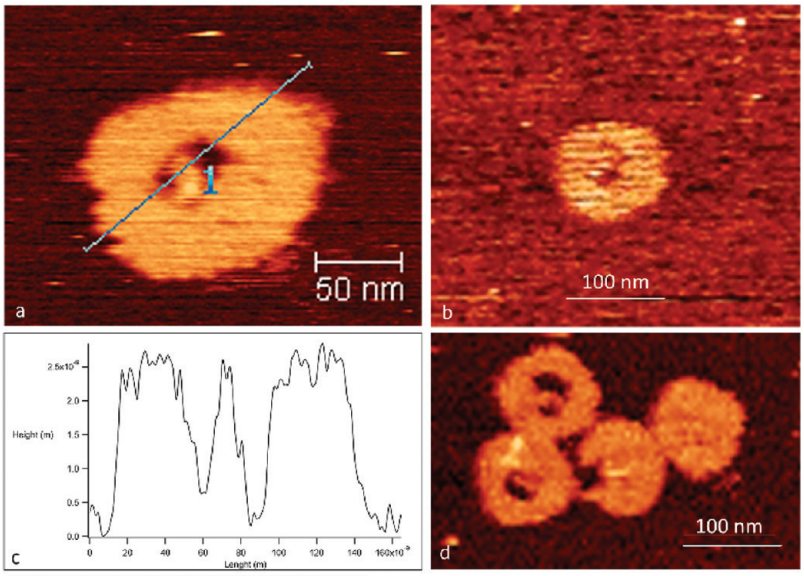

Figure 3. AFM imaging of DNA origami structures after hybridization with a complementary target. a), b) and d) AFM topographic images in tapping mode in liquid of well formed origami deposited on freshly cleaved mica surface. Two openings are evident and the origami structure resembles the cartoon shown in Figures 1c and d; c) height profile of the structure, referred to the line 1 in the AFM image in a, highlighting that the opening of the nanostructure reaches the substrates as expected for a complete opening.

conformation by moving the wing edges toward each other. The modification induced by the probe-target hybridization in the origami structure has been observed by AFM as shown in Figure 3a,b, where two openings separated by a ridge could be directly identified in real space, as expected from wing movement, and in accordance to the origami design.

We investigated the efficiency of the actuation by recording a number of AFM images and counting the number of reacted versus non reacted origami nanostructures. When the target was added to buffer-suspended origami, that is, before the deposition on the substrate, 86 ± 6% of the structures reacted with the target and changed conformation. When the origami was first deposited on the substrate and then exposed to the target solution, however only 48 ± 15% of the origami structures were found to be opened. Since to successfully hybridize with the target, the origami should lie on the substrate surface face-up, the two data are consistent; the

dx.doi.org/10.1021/nl203217m |*Nano Lett.* 2011, 11, 5449–5454

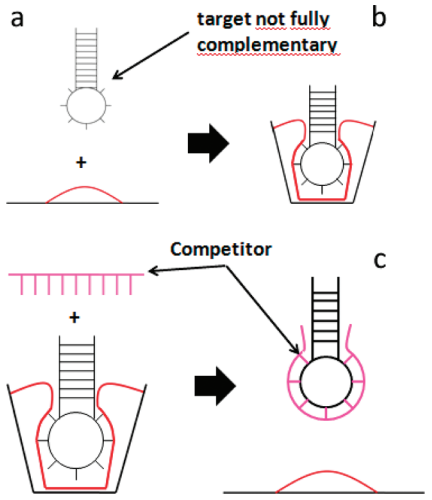

Figure 4. Base sequence schematics for the probe/target and target/competitor actuation system. Illustration of the reversible system concept. (a,b) The target (harpin) acts with a probe (red) that complements only on its terminal parts with the target T_m, leaving a mismatch of 34 nucleotides in the middle of the molecules. This not complemented site remains available for a third DNA molecule involved in the reversible switching process, the competitor (pink). (c) The 84 nts competitor is perfectly complementary to the target and, fueled by the free energy of base pair formation and starting from the 34 nucleotides mismatch, triggers the detach between target and probe. This hybridization event target/competitor turns off again the system due to the relaxation of the probe.

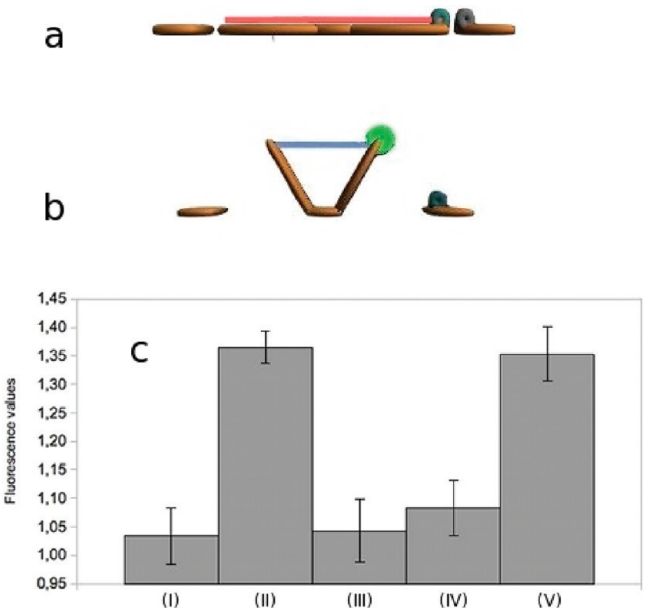

Figure 5. Principle and measures of the FRET detection of reversible actuation. (a) With the origami in the rest state fluorophore and quencher are within a Forster radius distance and there is no emission. (b) With the origami in the constrained state, the flourophore and the quencher are moved far away and light is emitted. (c) Fluorescence intensity (arbitrary units) emitted by a 1.6 nM solution of origami as synthesized (I), and after the addition of partially complementary target molecules (II) or after addition of a noncomplementary target used as a negative control (III). (IV) fluorescence intensity measured from the same reaction measured (II) after the addition of the competitor and (V) after the addition of a control competitor that was not complementary to the target. Each bar is the average of at least 20 independent measurements.

small difference between the observed (48%) and the expected (one-half of 86%) means, although within a statistical error, may be explained with a orientation preference when the origami are deposited on mica, as it has been reported before for other origami.[5] Moreover, our observations indicate that the actuation force is large enough to overcome the electrostatic and van der Waals interactions between the DNA origami actuator and the substrate, as well as the stacking between the internal disk and the external ring, demonstrating the applicability of our strategy for integration of DNA origami actuators with solid-state detectors and electronics. The force exerted depends on the formation of the probe/target hybrid pair that is constrained by the 18 bp GC clamp in the target hairpin. On the basis of the merasures on the hybridization and dehybridization forces and times on a 60bp RNA hairpin (n), we expect that in our systems the forces involved are in the 10pN regime and the DNA hybridization time is in the submillisecond regime, much shorter than the recognition time, that is, the time required for the target to find and get close enough to the probe in order to start the hybridization process.

To integrate a further degree of flexibility in our nanodevice, we next present a scheme for making the wing movement of the DNA origami actuator reversible, by using probe/target pairs that were not fully complementary. This design implied a first hybridization step between the probe DNA on the DNA origami and a partly complementary target for forward actuation that brings together the wings, forming two semicircular gaps in the origami center. The reverse actuation was performed by decomposing the probe/target hybrid by adding an excess amount of an additional oligonucleotide named the "competitor", which was perfectly complementary to the target. This perfect complementarity of target versus competitor ensured the target to be displaced from the probe and caused reversal of the origami to its original configuration.

The concept of the reversible switch is summarized in Figure 4. In Figure 4a, the origami switch is closed, the wings lay in the same plane of the external ring and the ssDNA probe is not hybridized. In Figure 4b, the partially complementary target binds to the probe inducing the wing motion. In Figure 4c, the fully complementary competitor binds to the target displacing the probe: the wings, which are no longer subject to the tensile force generated by the hybridization, relax to the initial conformation on the plane.

A fast and qualitative method based on insertion of a Förster resonance energy transfer (FRET) couple in the structure was introduced to monitor the conformation changes of the DNA origami associated with wing motion following the target addition. The DNA origami was assembled with a staple strand on the external edge of the internal disk labeled with a fluorophore (6′-FAM), and with an oligonucleotide on the internal edge of the external ring labeled with a quencher (BHQ-1). In the absence of the target, with the wings in the relaxed initial position a low intensity signal (bar I in Figure 5c) was detected since fluorophore and quencher were located within the Förster radius (~1 nm), as shown in Figure 5a. No variation in fluorescence intensity was recorded when a nontarget DNA was added to the origami suspension (bar III in Figure 5c). Conversely, when the wings were constrained following the addition of a probe hybridizing target, the consequent FRET separation resulted larger than 16 nm (Figure 5b) with a significant increase of fluorescent signal intensity. Bar II in Figure 5c shows the increase in fluorescence intensity recorded after the addition of a target partially complementary to the origami probe. Moreover, following further addition

dx.doi.org/10.1021/nl203217m |*Nano Lett.* 2011, 11, 5449–5454

of the competitor to the suspension of reacted origami, the fluorescence intensity returned to the initial value (bar IV) within the experimental error, demonstrating that the origami configuration was reverted. Parallel assays carried out with a competitor that was noncomplementary to the target produced no changes in fluorescence (bar V, Figure 5c).

In summary, we have successfully designed, constructed, and imaged a 100 nm-sized round DNA origami actuator capable of reversible motion in response to an external chemical stimulus. The development of complex nanosized objects, which acts as actuators in response to single molecule interaction, is an important step toward integration and automation of rapid and high throughput analysis with ultralow volume sample/reagent. In the design presented here, two wing tips that are >40 nm distant in the rest position are brought in close proximity after actuation, thus producing the longest travel produced by a molecular motor in a single reaction step ever reported. Although in this design the actuation is powered by a standard DNA−DNA hybridization, the substitution of the probe DNA with more complex DNA nanoconstructs would provide finely tunable and/or logically switchable movements.[16,17] In addition, the reversibility of the nanoactuator and the effectiveness of this actuation mechanism both with the origami in solution and when deposited on a 2D surface significantly multiplies the potential range of applications. By combining the stability and the high information density of the DNA origami nanostructure together with reversibility of actuation, we propose that the nanoactuator can be used as platform for addressing, moving and modifying nanomaterials. The nanoactuator can further be assembled into patterns with required directionality and thus potentially become able to guide matter or energy transfer when integrated with electrically active components. With the switchable functionalities we here have demonstrated, the DNA origami offers a genuine, versatile, and useful technology at hand for the future nanomaterial science, with endless possibilities within the emerging area of nanotechnology demonstrating that there is indeed plenty of room "at the bottom".

Materials and Methods. If not otherwise specified, all oligonucleotides were purchased standard purified form from Sigma-Aldrich (Germany), resuspended in water at 100 μM concentration and stored at −20 °C. All the solutions used were sterilized by autoclaving at 121 °C for 21 min. All the oligonucleotide sequences are reported in the Supporting Information (Table S1).

DNA Origami Design. The DNA origami design and prediction of the dimensions were made with the help of the software package named caDNAno square lattice software package.[18] The desired set of staple strands was mixed in a 10-fold excess (16 nM, except for oligonucleotides Linker dx, linker sx, CrI_{FRET}, DkD_{FRET}, used in a 1:1 ratio) with 1.6 nM circular M13mp18 DNA (New England Biolabs, Ipswich, MA) in 100 μL TAEM (10x TAEM solution is 125 mM $MgCl_2$, 400 mM Tris-HCl, 10 mM EDTA pH 8.0, 20 mM NaCl) and annealed from 95 to 25 °C in a PCR machine (Eppendorf) at a rate of 0.01 °C/s ramp. After annealing, the DNA origami was stored at 4 °C. Annealing products were run in a 0.7% agarose gel in 1x TAE at 75 V for 90 min.

Purification of Folded Samples. Folded constructs were purified from staple strands excess using Amicon Ultra 0.5 mL 100 kDa (Millipore, Massachusetts), adjusting the protocol supplied by the constructor. Briefly, 2× TAEM solution was added in the same amount of sample volume; capped Amicon Ultra were centrifuged four times for 1.5 min at 14 000g. Concentrated samples were eluted spinning the inverted filters in a clean vial at 2000g for 3 min.

Probe, Target, and Competitor. Sequences were drawn using the program BioEdit v.7.0.9[19] and were built using the rules of no self-annealing, no loops in each sequence, no strong dimers and 50% GC, that were checked using the online tools of IDT's Oligo Analyzer v.3.1.[20] An exception was made for the target as it includes a 18 bp GC clamp. To explore the functionality, the complexes probe/target and target/competitor were reacted with their complementary or partial complementary strands in equimolar proportion in a water 10 μM solution containing 1x TAEM. The solutions were heated at 95 °C for two minutes in a thermocycler and allowed to cool down at room temperature for two hours. Hybridization in this case was performed at room temperature for one hour. The probe ssDNA (1.6 nM) was linked to the origami in a 1:1 ratio, complementing the protruding oligonucleotides Linker dx and Linker sx.

When used for actuation, the target was added in a 100:1 concentration relative to the probe and allowed to react for 1 h at room temperature. In order to demonstrate reversion of the origami actuation, the origami was first actuated by adding a target, not perfectly matching the probe, in a 100:1 concentration relative to the probe; then the origami initial configuration was re-established by adding the competitor in a 10:1 concentration relative to the target. Origami configuration changes were monitored by FRET (see below).

FRET System. To detect the opening of the wings, the internal disk and the external ring were functionalized by substituting oligonucleotide DkD3 with the 6′-FAM labeled DkD_{FRET} and oligonucleotide CrI3 with the BHQ-1 labeled CrI_{FRET}. Oligonucleotides were purchased HPLC purified from MWG Operon, Ebersberg). DNA origami motion was directly monitored with a CCD detector (model AP47p, Apogee) mounted on a fluorescence microscopy (Leitz Orthoplan), analyzing 12 μL of sample illuminated with an exciting 470 nm blue emission and a 517−540 nm filter.

Nucleic Acids Visualization. Folded and purified DNA-based origami were electrophoresed on 0.7% (w/v) agarose gel (Pronadisa). Other DNA products as shorter ssDNA or dsDNA were run in a 3% (w/v) agarose gel. In all cases, gels were previously added of 0.5x Gel Red™ nucleic acid stain (Biotium, Hayward, CA) and run 1x TAE (for 200 mL of a 50x buffer solution: 400 mM Tris-HCl, 11.42 mL acetic acid, 20 mL EDTA 0.5 M, pH 8.0) for a time dependent voltage and then visualized and photographed under UV light.

Atomic Force Microscopy. Samples were dispersed on a freshly cleaved mica surface in a saline buffer (125 mM $MgCl_2$, 400 mM Tris-HCl, 10 mM EDTA, 20 mM NaCl, pH 8.0). The large concentration of positive ions, mainly Mg^{2+} has the functionality of screening the negative charges present at the mica surface and on the external structure of the dsDNA, allowing the adhesion of the origami nanostructures to the mica surface. Samples were let sediment for at least five minutes and were never rinsed or dried. The AFM Images have been recorded using either a JPK Nanowizard II, a VEECO Multimode with Nanoscope V control or an Asylum MFP3D AFM system. All the AFM instruments where operated in liquid in tapping mode. We used Olympus OMCL-TR400PSA tips with a force constant of 0.08 N/m and a resonance frequency of 34kHz, in air.

■ ASSOCIATED CONTENT

Supporting Information. Graphical model of the DNA origami, oligonucleotides sequences, more AFM images. This material is available free of charge via the Internet at http://pubs.acs.org.

AUTHOR INFORMATION

Corresponding Author

*Tel.: +39 0432558531. Fax: +39 0432558501. E-mail: firrao@uniud.it.

Present Addresses

¶Department of Physics, Middle East Technical University, Dumlupinar Bulvari 1, Universiteler Mahallesi, Cankaya, 06800 Ankara - Turkey.

ACKNOWLEDGMENT

This work was supported in part by PRIN, project 2008F2-F82F, granted to GF, in part was funded under European projects BINASP FP6-SSA011936 and SMD FP7-NMP 2800-SMALL-2 proposal no. CP-FP 229375-2. M.D. and F.B. would like to acknowledge the financial support from The Danish National Research Foundation, the Danish Research Council, the Carlsberg Foundation, and the European Research Council (ERC advanced Grant to F.B.).

REFERENCES

(1) Huang, T. J.; Juluri, B. K. *Nanomedicine.* **2008**, *3*, 107–24.

(2) Omabegho, T.; Sha, R.; Seeman, N. C. *Science* **2009**, *324*, 67–71.

(3) Lund, K.; Manzo, A. J.; Dabby, N.; Michelotti, N.; Johnson-Buck, A.; Nangreave, J.; Taylor, S.; Pei, R.; Stojanovic, M. N.; Walter, N. G.; Winfree, E.; Yan, H. *Nature* **2010**, *465*, 206–210.

(4) Seeman, N. C. *Nature* **2003**, *421*, 427–31.

(5) Rothemund, P. W. K. *Nature* **2006**, *440*, 297–302.

(6) Andersen, E. S.; Dong, M.; Nielsen, M. M.; Jahn, K.; Lind-Thomsen, A.; Mamdouh, W.; Gothelf, K. V.; Besenbacher, F.; Kjems, J. *ACS Nano* **2008**, *2*, 1213–8.

(7) Andersen, E. S.; Dong, M.; Nielsen, M. M.; Jahn, K.; Subramani, R.; Mamdouh, W.; Golas, M. M.; Sander, B.; Stark, H.; Oliveira, C. L. P.; Pedersen, J. S.; Birkedal, V.; Besenbacher, F.; Gothelf, K. V.; Kjems, J. *Nature* **2009**, *459*, 73–76.

(8) Douglas, S. M.; Dietz, H.; Liedl, T.; Högberg, B.; Graf, F.; Shih, W. M. *Nature* **2009**, *459*, 414–8.

(9) Subramani, R.; Jensen, S. J.; Rotaru, A.; Andersen, F. F.; Gothelf, K. V.; Mamdouh, W.; Besenbacher, F.; Dong, M.; Knudsen, B. R. *ACS Nano* **2010**, *4*, 5969–77.

(10) Voigt, N. V.; Tørring, T.; Rotaru, A.; Jacobsen, M. F.; Ravnsbaek, J. B.; Subramani, R.; Mamdouh, W.; Kjems, J.; Mokhir, A.; Besenbacher, F.; Gothelf, K. V. *Nat. Nanotechnol.* **2010**, *5*, 200–3.

(11) Ding, B.; Wu, H.; Xu, W.; Zhao, Z.; Liu, Y.; Yu, H.; Yan, H. *Nano Lett.* **2010**, *10*, 5065–5069.

(12) Ding, B.; Deng, Z.; Yan, H.; Cabrini, S.; Zuckermann, R. N.; Bokor, J. *J. Am. Chem. Soc.* **2010**, *132*, 3248–9.

(13) Pal, S.; Deng, Z.; Ding, B.; Yan, H.; Liu, Y. *Angew. Chem., Int. Ed.* **2010**, *49*, 2700–4.

(14) Kuzuya, A.; Koshi, N.; Kimura, M.; Numajiri, K.; Yamazaki, T.; Ohnishi, T.; Okada, F.; Komiyama, M. *Small.* **2010**, *6*, 2664–7.

(15) Dietz, H.; Douglas, S. M.; Shih, W. M. *Science* **2009**, *325*, 725–30.

(16) Zhang, Z.; Olsen, E. M.; Kryger, M.; Voigt, N. V.; Tørring, T.; Gultekin, E.; Nielsen, M.; MohammadZadegan, R.; Andersen, E. S.; Nielsen, M. M.; Kjems, J.; Birkedal, V.; Gothelf, K. V. *Angew. Chem., Int. Ed.* **2011**, *50*, 3983–7.

(17) Bath, J.; Turberfield, A. J. *Nat. Nanotechnol.* **2007**, *2*, 275–84.

(18) Douglas, S. M.; Marblestone, A. H.; Teerapittayanon, S.; Vazquez, A.; Church, G. M.; Shih, W. M. *Nucleic Acids Res.* **2009**, *37*, 5001–6.

(19) Hall, T. *Nucleic Acids Symp. Ser.* **1999**, *41*, 95–8.

(20) Owczarzy, R.; Tataurov, A. V.; Wu, Y.; Manthey, J. A.; McQuisten, K. A.; Almabrazi, H. G.; Pedersen, K. F.; Lin, Y.; Garretson, J.; McEntaggart, N. O.; Sailor, C. A.; Dawson, R. B.; Peek, A. S. *Nucleic Acids Res.* **2008**, *36*, W163–9.